Comprehensive Psychoneuroendocrinology 4 (2020) 100013

Contents lists available at ScienceDirect

Comprehensive Psychoneuroendocrinology

journal homepage: www.elsevier.com/locate/cpnec

# Adipose PTEN acts as a downstream mediator of a brain-fat axis in environmental enrichment

Wei Huang [a,b,1], Nicholas J. Queen [a,b,1], Travis B. McMurphy [a,b], Seemaab Ali [a,b], Ryan K. Wilkins [a,b], Bhavya Appana [a,b], Lei Cao [a,b,*]

[a] Department of Cancer Biology & Genetics, College of Medicine, The Ohio State University, Columbus, OH, 43210, USA
[b] The Ohio State University Comprehensive Cancer Center, Columbus, OH, 43210, USA

ARTICLE INFO

*Keywords:*
Environmental enrichment
PTEN
Adipose tissue
Sympathetic nervous system
Lipolysis
AAV

ABSTRACT

*Background/Objectives:* Environmental enrichment (EE) is a physiological model to investigate brain-fat interactions. We previously discovered that EE activates the hypothalamic-sympathoneural adipocyte (HSA) axis via induction of brain-derived neurotrophic factor (BDNF), thus leading to sympathetic stimulation of white adipose tissue (WAT) and an anti-obesity phenotype. Here, we investigate whether PTEN acts as a downstream mediator of the HSA axis in the EE.

*Methods:* Mice were housed in EE for 4- and 16-week periods to determine how EE regulates adipose PTEN. Hypothalamic injections of adeno-associated viral (AAV) vectors expressing BDNF and a dominant negative form of its receptor were performed to assess the role of the HSA axis in adipose PTEN upregulation. A β-blocker, propranolol, and a denervation agent, 6-hydroydopamine, were administered to assess sympathetic signaling in the observed EE-PTEN phenotype. To determine whether inducing PTEN is sufficient to reproduce certain EE adipose remodeling, we overexpressed PTEN in WAT using an AAV vector. To determine whether adipose PTEN is necessary for the EE-mediated reduction in adipocyte size, we injected a rAAV vector expressing Cre recombinase to the WAT of adult $PTEN^{flox}$ mice and placed the mice in EE.

*Results:* EE upregulated adipose PTEN expression, which was associated with suppression of AKT and ERK phosphorylation, increased hormone-sensitive lipase (HSL) phosphorylation, and reduced adiposity. PTEN regulation was found to be controlled by the HSA axis—with the hypothalamic BDNF acting as the upstream mediator—and dependent on sympathetic innervation. AAV-mediated adipose PTEN overexpression recapitulated EE-mediated adipose changes including suppression of AKT and ERK phosphorylation, increased HSL phosphorylation, and reduced adipose mass, whereas PTEN knockdown blocked the EE-induced reduction of adipocyte size.

*Conclusions:* These data suggest that adipose PTEN responds to environmental stimuli and serves as downstream mediator of WAT remodeling in the EE paradigm, resulting in decreased adipose mass and decreased adipocyte size.

## Introduction

Adiposity is determined by the balance between fat storage and release within adipose tissue. Like many other biological processes, adiposity is regulated through various homeostatic phenomena; a neural-adipose axis serves as one mediator of such mechanisms [1,2]. The hypothalamus is a central driver of energy homeostasis, acting to induce local and systemic metabolic change via sympathetic innervation to adipose tissue. Physiological challenges—including cold exposure and exercise—have been shown to activate this neural-adipose axis for homeostatic maintenance [3,4]. Genetic, environmental, and behavioral factors are all thought to play a role in whole-body adipose homeostasis [5].

Environmental enrichment (EE) serves as one additional physiological stimulation model to induce metabolic remodeling in rodents. This experimental paradigm utilizes a complex, stimulating housing

* Corresponding author. Department of Cancer Biology and Genetics College of Medicine The Ohio State University Columbus, OH, 43210, USA.
*E-mail address:* lei.cao@osumc.edu (L. Cao).
[1] These authors contributed equally to this work.

https://doi.org/10.1016/j.cpnec.2020.100013
Received 30 September 2020; Accepted 14 October 2020

environment [6,7] to induce profound changes in neural function [8] and systemic metabolism [1,2]. Our lab uses EE to study how complex physical and social environments modulate metabolic, immune, and behavioral health and how environmental factors influence various disease models, including metabolic syndrome and cancer [1,2,6,7,9–14].

EE activates the hypothalamic-sympathoneural adipocyte (HSA) axis via induction of brain-derived neurotrophic factor (BDNF) [1]. Hypothalamic BDNF upregulation—whether through environmental or genetic means—leads to preferential activation of sympathetic tone to the white adipose tissue (WAT) and β-adrenergic signaling [1]. Accordingly, adipose tissue is a reliable responder to the EE experimental paradigm. EE-induced metabolic remodeling is characterized by reduced adiposity, lower circulating leptin, and improved glycemic control. EE enhances adipose vascular endothelial growth factor (VEGF) signaling and induces beige cells, contributing to increases in energy expenditure and adaptive thermogenesis [1,15]. Our lab has characterized the robust and repeatable EE metabolic phenotype across various murine models, including: normal chow-fed wild type [1,2], diet-induced obesity [1,2,9,16], aged [13,17], and autism spectrum disorder-like BTBR mice [14].

Phosphatase and tensin homolog deleted on chromosome ten (PTEN) has dual roles, serving as a tumor suppressor [18] and lipid phosphatase [19]. The latter role implicates PTEN as a player in adipose remodeling processes. Indeed, loss- and gain-of-function studies in genetically modified mouse models suggest that PTEN plays a pivotal role in developing mature adipose tissue, serving to modulate the size and/or mass of adipocytes and thereby fat distribution [20–24]. We recently reported that adipose PTEN regulates adult adipose tissue distribution through an adipose PTEN-leptin-sympathetic loop [25]. Moreover, previous reports suggest that global overexpression of PTEN contributes toward increased longevity, improved metabolism, and the development of anti-obesity and anti-cancer states [23,24]. Additionally, similar results have been observed in fat-specific insulin receptor knock-out (FIRKO) mice [26–28]. EE confers many of these same physiological benefits across various murine models [7], leading us to explore whether EE regulates adipose PTEN expression and how PTEN modulation contributes to the EE-induced WAT remodeling process.

Recently, we characterized a novel engineered hybrid serotype adeno-associated virus (AAV): Rec2 (AAV-Rec2) that achieves superior transduction of adipose tissue than the natural occurring AAV serotypes. We and others have applied the Rec2 serotype vectors to manipulate fat depots of interest in various mouse models [29–33]. Furthermore, a dual-cassette vector design has been introduced to achieve highly selective transduction of visceral fats while severely restricting off-target transduction of liver by intraperitoneal administration [30,34]. Here, we used this unique delivery system to investigate the role of adipose PTEN in EE-induced adipose remodeling.

## Materials and methods

### *Mice*

C57BL/6 mice were purchased from Charles River Laboratories (Wilmington, MA) and were used for the preliminary EE experiments (Fig. 1 and Fig. 2), HSA axis experiments (Fig. 3A, B, 3D, 3E, and 3F) and PTEN overexpression experiments (Fig. 4). BDNF heterozygous mice were previously provided by Dr. F. Lee of Weill Medical College of Cornell University and were bred in the animal facilities at The Ohio State University (Fig. 3C). PTEN$^{flox}$ mice on a C57BL/6 background (stock no: 006440) were purchased from The Jackson Laboratory (Bar Harbor, ME) and were subsequently bred in-house for the EE-PTEN WAT knockdown experiment (Figs. 5 and 6). Our previous work indicated that local manipulation of PTEN is efficacious in both sexes [25], thus both sexes were used in this experiment to maximize animal utility.

### *EE protocol*

Mice were housed in large EE cages (20 cm × 90 cm x 76 cm with 10 mice per cage for the initial EE experiments in Figs. 1 and 2; 63 cm × 49 cm x 44 cm with 3–5 mice per cage for WAT-directed PTEN knockdown in Figs. 5 and 6) supplemented with running wheels (one wheel in mid-size cage; 2–3 wheels in large cage), maze tunnels, huts, retreats, wood logs, and nesting material in addition to chow diet and water as previously described [1,6]. EE cage arrangements were varied on a weekly basis. Control mice were housed within standard laboratory environment (SE) cages of 30.5 cm × 17 cm x 15 cm (3–5 mice per cage). For the EE experiments, mice were exposed to EE for 4- and 16-week periods. Male

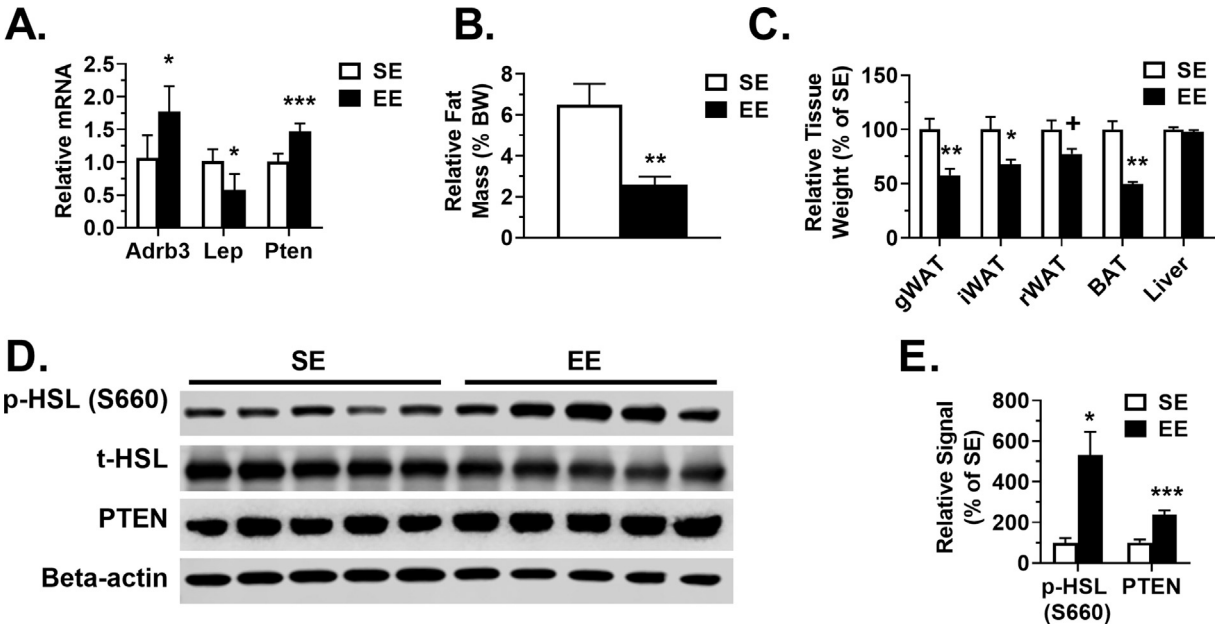


**Fig. 1. 4-week EE induces PTEN in WAT.** (A) Gene expression profile of the gWAT after 4 weeks in SE or EE housing (n = 5 per group). (B) Relative whole-body fat mass after 4 weeks of housing (n = 9 SE and n = 8 EE). (C) Relative tissue weight at sacrifice (n = 5 per group). (D) Western blots of gWAT lysates (n = 5 per group). (E) Protein quantification of gWAT lysates (n = 5 per group). Data are means ± SEM. + P < 0.10, *P < 0.05, **P < 0.01, ***P < 0.001.

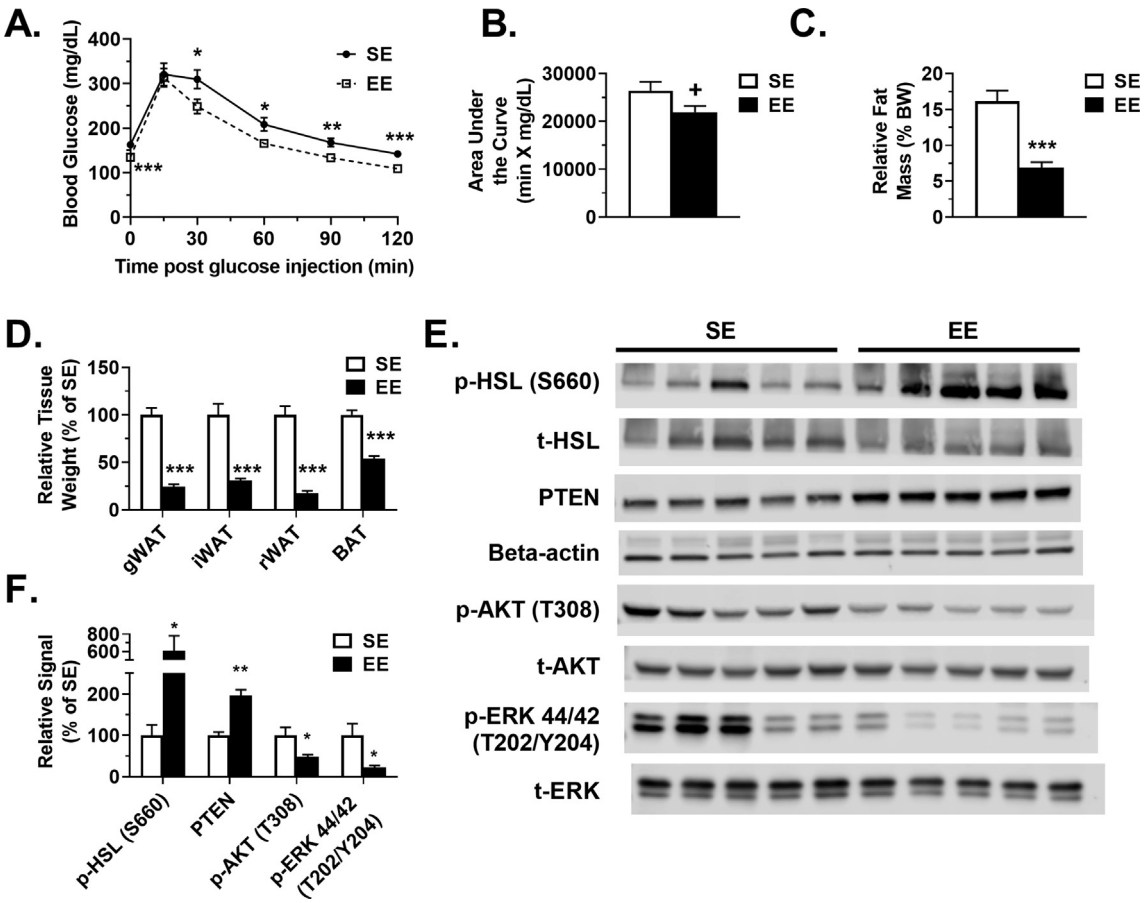


**Fig. 2. 16-week EE induces PTEN in WAT.** (A) Glucose tolerance test at 14 weeks post housing (n = 10 per group). (B) Area under the curve from (A) (n = 10 per group). (C) Adiposity by echoMRI at 15 weeks post housing (n = 10 per group). (D) Relative tissue weight at sacrifice (n = 10 per group). (E) Western blots of gWAT lysates (n = 5 per group). (F) Protein quantification of gWAT lysates (n = 5 per group). Data are means ± SEM. + P < 0.10, *P < 0.05, **P < 0.01, ***P < 0.001.

5-week-old C57BL/6 mice were used for the 4-week-long EE experiment. Male 3-week-old C57BL/6 mice were used for the 16-week-long EE experiment. Young adult female PTEN$^{flox}$ mice were used for the PTEN knockdown experiment; mice were housed in EE or SE for 4 weeks. Our previous work indicated that EE is efficacious in both sexes [2,9,11–13,15], thus both sexes were used in this experiment to maximize animal utility.

*rAAV vector construction and packaging*

The rAAV cis plasmid used in these experiments contained a vector expression cassette consisting of the CMV enhancer and chicken β-actin (CBA) promoter, woodchuck post-transcriptional regulatory element (WPRE) and bovine growth hormone poly-A flanked by AAV2 inverted terminal repeats. Cre recombinase and PTEN transgenes were inserted into the multiple cloning sites between the CBA promoter and WPRE sequence. Human TrkB isoform 1 (TrkB.T1), human BDNF, or destabilized YFP transgenes were inserted into the multiple cloning sites between the CBA promoter and WPRE sequence. rAAV serotype AAV1 vectors for TrkB.T1, YFP, or BDNF were packaged and purified as described elsewhere [35]. rAAV serotype Rec2 vectors for Cre recombinase and mouse PTEN included a second cassette encoding a microRNA driven by basic albumin promoter to limit transgene expression in the liver. This liver-restricting dual-cassette was previously described and verified elsewhere [30]. The empty control vector lacked a transgene insertion in the multiple cloning sites. Rec2 serotype specificity, transduction efficacy in adipose tissue, and packaging were previously detailed elsewhere [29,36].

*PTEN overexpression in the visceral adipose tissues*

Six-week-old male C57BL/6 mice were administered Rec2-PTEN or Rec2-Empty intraperitoneally ($2.0 \times 10^{10}$ vg diluted in 100 μL AAV-buffer) as previously described [30]. Mice were housed in SE and euthanized 4 weeks and 8 weeks post AAV injection for tissue and serum collection. Sacrifice occurred following a 4-h fast.

*Knockdown of adipose PTEN in EE*

Female PTEN$^{flox}$ C57BL/6 mice were randomized to receive an IP injection ($1.5 \times 10^{10}$ vg) of either a vector containing a Cre recombinase transgene (Rec2-Cre) or a control vector lacking the transgene (Rec2-Empty). Mice underwent surgery and skin was cut to reveal subcutaneous iWAT tissue as previously described [37]. Mice were administered direct iWAT injections ($1.0 \times 10^{10}$ vg/fat depot) of either Rec2-Cre or Rec2-Empty (Fig. 5A). Following two weeks of surgical recovery, mice were placed in either SE or EE housing. After four weeks of housing, mice were sacrificed.

*Statistical analysis*

Data are expressed as means ± SEM. Microsoft Excel, IBM SPSS v.25, and GraphPad Prism 8 software were used to analyze data. The Student's *t*-test was utilized for comparisons between two groups. Two-way ANOVAs with Tukey's *post hoc* correction were used for experiments with 2 × 2 design. GTT time course data were analyzed using a mixed ANOVA. Normality was tested using the Shapiro-Wilk method.

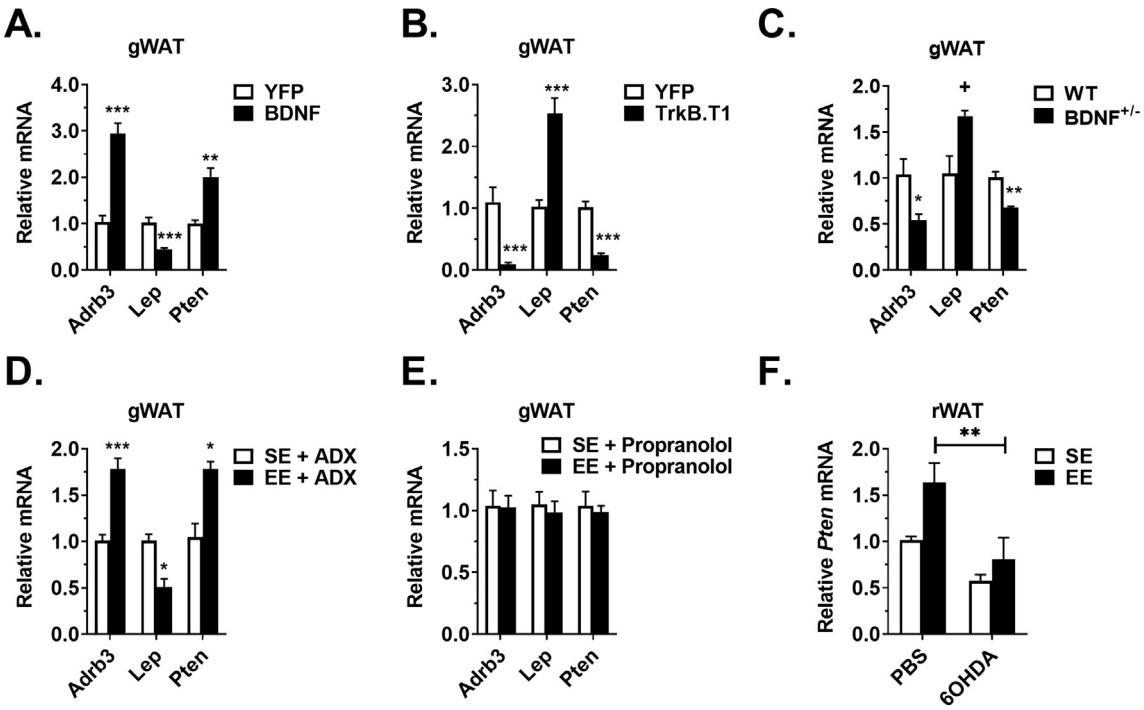


**Fig. 3. HSA axis regulates *Pten* expression in WAT.** (A) Gene expression profile of the gWAT in hypothalamic BDNF overexpression experiment (n = 5 per group). (B) Gene expression profile of the gWAT in rAAV-TrkB.T1 hypothalamically-injected mice (n = 5 per group). (C) Gene expression profile of the gWAT in BDNF $^{\pm}$ mice (n = 4 per group). (D) Gene expression profile of the gWAT in adrenalectomized mice after 5 weeks in SE or EE housing (n = 5 per group). (E) Gene expression profile of the gWAT in mice treated with oral propranolol 5 weeks in SE or EE housing (n = 5 per group). (F) *Pten* expression within rWAT in SE or EE mice treated with 6OHDA denervation agent (n = 5 per group). Data are means ± SEM. + P < 0.10, *P < 0.05, **P < 0.01, ***P < 0.001.

Additional Materials and Methods are in Supplementary Information.

## Results

### *EE induces PTEN expression in WAT*

To determine whether adipose PTEN could be regulated via EE, we first examined gonadal WAT (gWAT) samples obtained from previously published work that reported EE reduced adiposity, adipocyte size, and serum leptin levels [1]. EE housing significantly upregulated *Pten* mRNA expression in the gWAT ($p < 0.001$), and additionally upregulated *Adrb3* (encoding β3 adrenoreceptor; $p = 0.046$) and downregulated *Lep* (encoding leptin; $p = 0.020$) (Fig. 1A). These findings were consistent with previous reports by our lab [1,2].

Next, we performed two additional EE experiments to examine adipose PTEN in the context of EE. During the first 4-week-long experiment, *in vivo* echoMRI imaging revealed that EE reduced relative fat mass (Fig. 1B; $p = 0.005$) without altering total body mass (Supplementary Fig. 1A). Relative lean mass was found to be unaffected (Supplementary Fig. 1B). At sacrifice, 4-week EE mice displayed a reduced relative tissue weight in various adipose depots, including gWAT ($p = 0.009$), inguinal white adipose tissue (iWAT; $p = 0.046$), retroperitoneal adipose tissue (rWAT; $p = 0.054$), and brown adipose tissue (BAT; $p = 0.002$) (Fig. 1C). Many of these results were consistent with previous reports by our lab [1]. Western blots of gWAT showed that EE increased adipose PTEN protein levels ($p = 0.018$) and phosphorylation of hormone-sensitive lipase (HSL S660; $p < 0.001$) (Fig. 1D and E).

A 16-week EE experiment showed similar results. Of note, in some measures, a longer period of EE increased the magnitude of metabolic improvement. An intraperitoneal glucose tolerance test (GTT) performed at 14 weeks post housing showed that EE led to improved systemic glucose disposal (Fig. 2A, $F_{1,18} = 5.85$, $p = 0.026$; Fig. 2B, $p = 0.063$). An *in vivo* echoMRI performed at 15 weeks post housing revealed that EE decreased relative fat mass (Fig. 2C; $p < 0.001$) and increased relative lean mass (Supplementary Fig. 1C; $p < 0.001$) with no concurrent change in total body weight (Supplementary Fig. 1D). At sacrifice, the 16-week EE cohort exhibited reduced relative tissue weight in the gWAT, iWAT, rWAT, and BAT fat depots (Fig. 2D; all $p < 0.001$). Western blots of gWAT tissue showed EE increased both PTEN protein levels ($p = 0.001$) and phosphorylation of HSL (S660; $p = 0.043$) (Fig. 2E and F). In addition, phosphorylation of both AKT (T308; $p = 0.049$) and ERK 44/42 (T202/Y204; $p = 0.048$) was reduced within EE gWAT (Fig. 2E and F). The observed decrease in phosphorylation of AKT (T308) may result from the induction of PTEN, as PTEN is a negative regulator of the AKT signaling pathway [19].

Previous work by our lab indicated that EE-mediated adipose remodeling occurs via HSA axis activation, which is characterized by increased sympathetic outflow to adipose tissue and increased β-adrenergic signaling [1]. Combined with our previous work, these newly obtained data suggest that EE may upregulate adipose PTEN expression via β-adrenergic receptor activation, promoting lipolysis and reduced adiposity.

### *HSA axis mediates EE-induced adipose Pten upregulation*

We next investigated whether adipose PTEN induction is mediated by the HSA axis. All WAT samples described in this section originated from our previous work [1,10,15] and were newly analyzed for this study.

To determine whether the HSA axis was implicit in adipose PTEN upregulation, we performed several genetic manipulations at the root of this neural-adipose axis. Hypothalamic BDNF acts as an upstream activator of the HSA axis [1]; accordingly, we injected a rAAV1 vector harboring human *BDNF* to the hypothalamus and housed the mice in the SE [1]. Destabilized yellow fluorescent protein (YFP) was similarly packaged and administered as a control. Hypothalamic *BDNF* overexpression induced *Pten* ($p = 0.001$) and *Adrb3* mRNA expression ($p <$

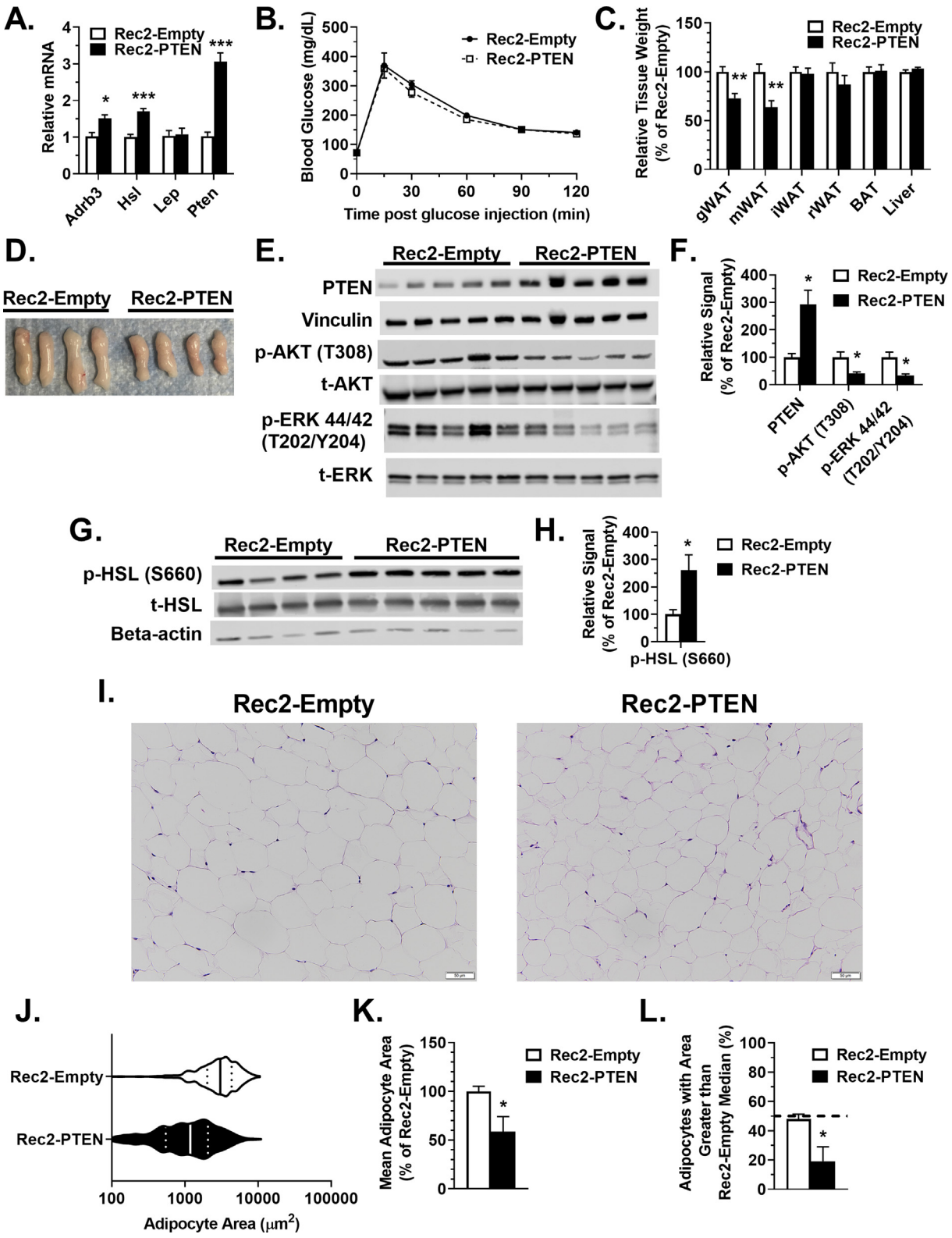


**Fig. 4. PTEN overexpression leads to reduced mass of targeted fat depot and adipocyte size.** (A) Gene expression profile of gWAT at 4 weeks post injection of Rec2-Empty or Rec2-PTEN (n = 5 per group). (B) Glucose tolerance test at 8 weeks post AAV injection (n = 5 per group). (C) Relative tissue weight at sacrifice (n = 10 per group). (D) Representative picture of gWAT depots. (E) Western blots of PTEN, p-AKT, and p-ERK 44/42 (T202/Y204) from gWAT lysates (n = 5 per group). (F) Quantification of western blots in (E) (n = 5 per group). (G) Western blot of p-HSL from gWAT lysates (n = 4 Rec2-Empty and n = 5 Rec-PTEN). (H) Quantification of western blots in (G). (I) Representative H&E images of gWAT. (J) Adipocyte area distribution curve with measures of interquartile range (n = 4 animals per group; 6 images analyzed per animal). (K) Mean adipocyte area (mean area of all adipocytes analyzed per animal; n = 4 animals per group). (L) Measure of the median adipocyte area (median area of all adipocytes analyzed per animal; n = 4 animals per group). Unless otherwise noted, data are means ± SEM. + $P < 0.10$, *$P < 0.05$, **$P < 0.01$, ***$P < 0.001$.

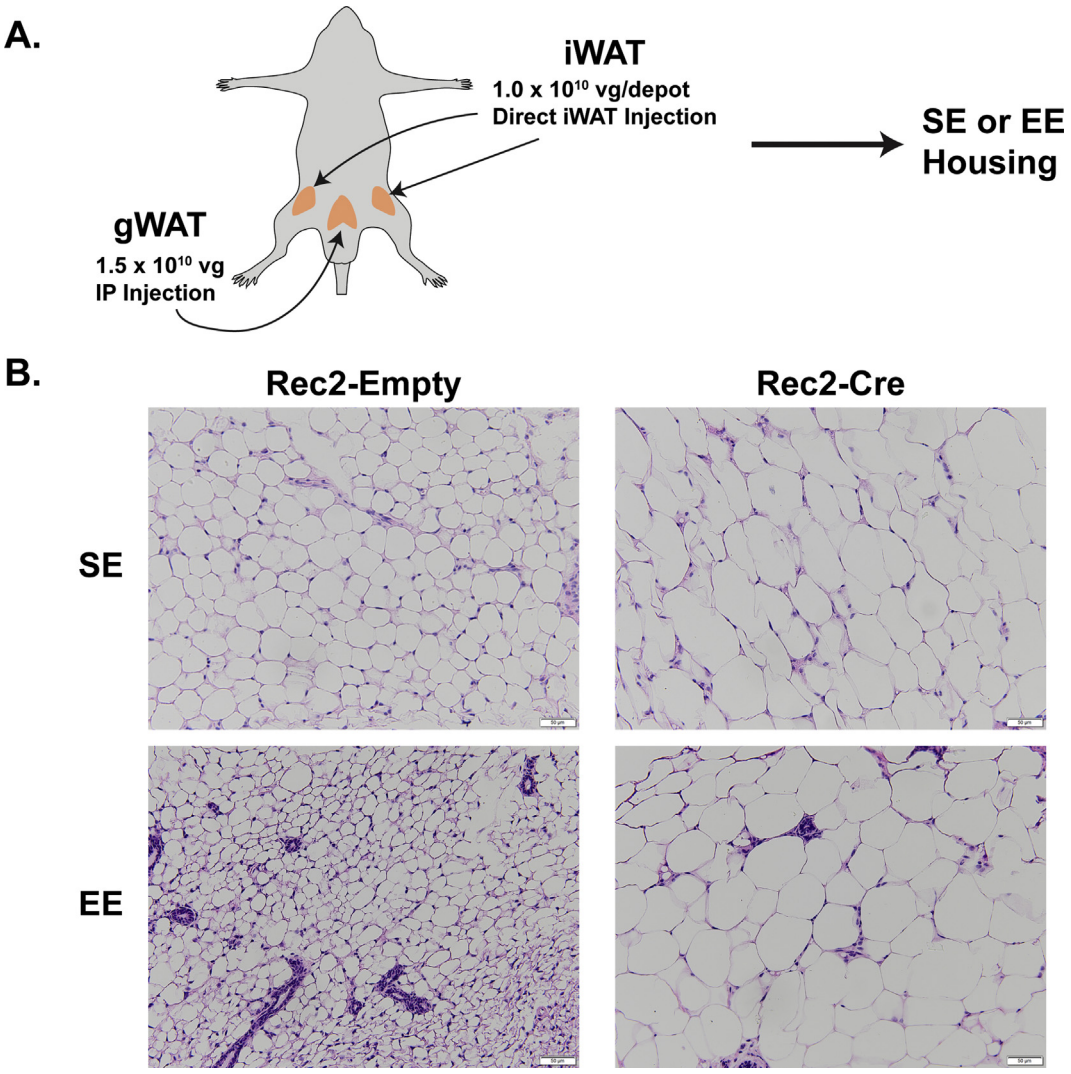


**Fig. 5. EE PTEN knockdown experiment design and representative images of iWAT.** (A) Schematic for the experiment design. (B) Representative H&E images of iWAT.

0.001) in the gWAT, while *Lep* mRNA expression ($p < 0.001$) was suppressed. As expected, hypothalamic BDNF overexpression reproduced the adipose phenotype induced by EE, including *Pten* upregulation (Fig. 3A). Next, we injected a rAAV1 vector delivering the dominant negative truncated form of the high-affinity BDNF receptor—tropomyosin-related kinase B (TrkB.T1)—to the hypothalamus, specifically antagonizing BDNF signaling in the hypothalamus [1]. The inhibition of hypothalamic BDNF signaling robustly downregulated gWAT *Pten* and *Adrb3* mRNA expression, while *Lep* mRNA expression was increased (Fig. 3B; $p < 0.001$ for all)—a complete reversal to the changes observed in EE or BDNF overexpressing mice. A similar pattern was observed (Fig. 3C; *Pten* $p = 0.006$, *Adrb3* $p = 0.026$, *Lep* $p = 0.061$) in heterozygous BDNF-deficient mice, whose BDNF level is approximately 40% lower than wild type [38].

Our recent studies indicate that the hypothalamic-pituitary-adrenal (HPA) axis is required for certain immune phenotypes associated with EE. For example, adrenalectomized animals did not display thymic changes in response to EE [10]. We assessed the gene expression profile of gWAT from the adrenalectomy study. Despite the lack of adrenal glands, EE remained effective on induction of *Pten* ($p = 0.016$) and *Adrb3* mRNA expression ($p < 0.001$) while downregulating *Lep* mRNA expression ($p = 0.016$) (Fig. 3D), suggesting neuronal action as the primary mediator of the PTEN-EE phenotype instead of adrenal catecholamine actions.

To determine the necessity of the sympathetic nervous system (SNS) for EE to upregulate PTEN in WAT, we administered the β-blocker propranolol to animals housed in EE [1]. Propranolol treatment blocked the effects of EE on WAT PTEN gene expression (Fig. 3E), indicating the essential involvement of the SNS for EE-induced PTEN upregulation. To assess the requirement of direct sympathetic stimulation for EE-induced PTEN upregulation, chemical denervation of the rWAT was performed prior to assigning animals to SE or EE conditions [15]. 6OHDA was injected directly to the rWAT to disrupt sympathetic innervation on WAT while leaving systemic SNS function intact. 6OHDA treatment significantly decreased *Pten* expression in the rWAT in animals housed in SE and completely abolished the ability of EE to upregulate *Pten* expression (Fig. 3F; $p = 0.009$). Combined with the hypothalamic manipulation studies, these data suggest that upregulation of PTEN in WAT occurs via the activation of the HSA axis.

### *PTEN overexpression in WAT reduces adipocyte size*

We established that EE induces PTEN in the WAT and that this upregulation occurs as a result of HSA axis activation. Our data raised the possibility that PTEN may serve as a downstream effector in EE-mediated adipose tissue remodeling. Accordingly, we sought to determine whether

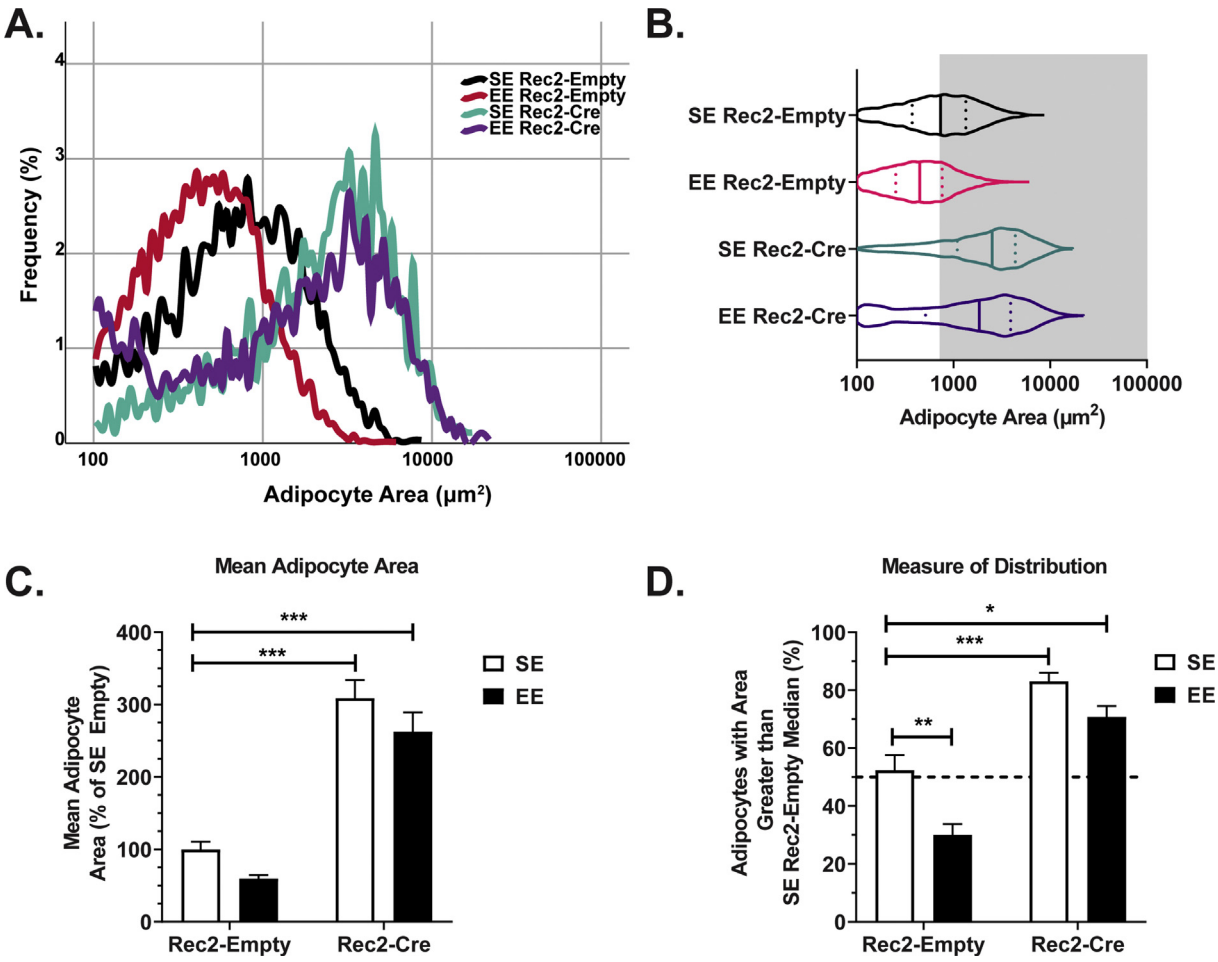


**Fig. 6. PTEN knockdown in WAT blocks EE-induced reduction in adipocyte size.** (A) Adipocyte area distribution curve (n = 6 animals per group; 6 images analyzed per animal). (B) Adipocyte area distribution curve with measures of interquartile range (n = 6 animals per group; 6 images analyzed per animal). (C) Mean adipocyte area (mean area of all adipocytes analyzed per animal; n = 6 animals per group). (D) Measure of the median adipocyte area (median area of all adipocytes analyzed per animal; n = 6 animals per group). Unless otherwise noted, data are means ± SEM. + P < 0.10, *P < 0.05, **P < 0.01, ***P < 0.001.

overexpression of PTEN in WAT could recapitulate some phenotypic changes associated with EE. To do so, we used our dual-cassette rAAV vector [30] to overexpress PTEN preferentially in visceral WAT. Using this construct, we previously investigated off-target transgene expression and found minimal expression in the liver, intestines, spleen, kidney, and testes [30].

Wild-type C57BL/6 mice were randomized to receive a single IP injection of either Rec2-PTEN ($2.0 \times 10^{10}$ vg) or a control vector lacking the transgene, Rec2-Empty. At 4 weeks post rAAV injection, half of the mice were sacrificed to assess transgene expression. gWAT samples from Rec2-PTEN mice exhibited upregulation of *Adrb3* (p = 0.012), *Hsl* (p < 0.001), and *Pten* (p < 0.001) mRNA expression, while *Lep* remained unchanged (Fig. 4A). Changes in gross tissue weights were not observed at this early time point (data not shown). The remaining mice were subjected to an intraperitoneal GTT at 8-weeks post viral injection. No change in glucose disposal was observed (Fig. 4B). At sacrifice, we observed that Rec2-PTEN led to a significant reduction in relative gWAT tissue weight (Supplementary Fig. 2; p = 0.003).

The adipose PTEN overexpression experiment was repeated in a second cohort and mice were carried to an 8-week time point. No changes in body weight or food intake were observed (data not shown). At sacrifice, we observed that Rec2-PTEN significantly reduced gWAT (Fig. 4C and D; p = 0.002) and mesenteric WAT (mWAT) relative tissue weight (Fig. 4C; p = 0.002). Western blotting of gWAT lysates confirmed PTEN overexpression (Fig. 4E and F; p = 0.017). Furthermore, PTEN overexpression suppressed phosphorylation of both AKT (T308; p = 0.036) and ERK 44/42 (T202/Y204; p = 0.018) (Fig. 4E and F) and increased phosphorylation of HSL (S660; p = 0.043) (Fig. 4G and H).

H&E staining was performed to assess changes in gWAT adipocyte morphology (Fig. 4I). Adipocyte size was quantified using computer software as previously described [25]. PTEN overexpression resulted in reduced adipocyte size, which was observed by a shift in the adipocyte area distribution curve (Fig. 4J) and a reduction in the mean adipocyte area (Fig. 4K; p = 0.049). A comparison of adipocyte median area additionally confirmed these findings (Fig. 4L; p = 0.027). Taken together, these data indicate that adipose PTEN overexpression—independent of housing environment—was sufficient to recapitulate some aspects of EE adipose phenotype, including reduced adiposity and adipocyte size, and increased lipolysis.

### *PTEN knockdown in WAT blocks EE-induced reduction in adipocyte size*

We recently reported that PTEN knockdown in mature adipose tissue leads to enlargement of the affected adipose depots and increased adipocyte size [25]. Given the observation of upregulation of PTEN and reduced adipose depot size in EE, we investigated whether PTEN knockdown could block or attenuate EE-induced adipose remodeling.

To functionally knock down PTEN, we introduced an adipose-specific AAV vector to the gWAT and iWAT as previously described [25,37]. To target the gWAT, $PTEN^{flox}$ mice were randomized to receive an IP

injection ($1.5 \times 10^{10}$ vg) of either a vector containing a Cre recombinase transgene (Rec2-Cre) or Rec2-Empty. The same mice were surgically administered direct iWAT injections ($1.0 \times 10^{10}$ vg/fat depot) of either Rec2-Cre or Rec2-Empty (Fig. 5A). Following two weeks of surgical recovery, mice were placed in either SE or EE housing to determine whether adipose PTEN knockdown affects EE-mediated changes in adipose tissue.

H&E staining was performed to assess changes in WAT adipocyte morphology (Fig. 5B). Adipocyte area distribution curves were generated (Fig. 6A and B). Mean and median adipocyte area are two measures to examine changes of adipocyte size. Both must be considered in tandem to fully appreciate changes in adipocyte biology. Full statistical comparisons are available in Supplementary Table 1. As expected, EE Rec2-Empty mice showed a reduction in adipocyte size when compared to their SE Rec2-Empty counterparts (Fig. 6A, B, and 6D; $p = 0.0043$ in Fig. 6D). Consistent with our previous publication [25], PTEN knockdown via Rec2-Cre resulted in increased adipocyte size (Fig. 6A–D; Fig. 6C virus main effect $F_{1,20} = 113.7$, $p < 0.001$, Fig. 6D virus main effect $F_{1,20} = 79.22$, $p < 0.001$). Notably, EE Rec2-Cre mice exhibited massively expanded adipocytes (Fig. 6C, $p < 0.001$; Fig. 6D, $p < 0.001$), and the EE-induced reduction of adipocyte size observed in Rec2-Empty treated mice was substantially attenuated in mice treated with Rec2-Cre (Fig. 6A–D). These results indicate adipose PTEN is required for the EE-mediated reduction in adipocyte size.

## Discussion

Our lab and others have sought to characterize an EE-driven regulatory network which encompasses multiple organ systems, including the central nervous, endocrine, and immune systems. Importantly, all of the above play a role in stress responses to physical and social environments. EE is considered to be a eustress—positive stress—model which activates both the HPA and HSA axes to induce improved metabolic, immune, and behavioral health [7,39–42]. Some have proposed EE induces a form of stress inoculation; within EE, environmental stressors are mild, predictable and easily manageable by animals to provide protection against future more severe stressors [43,44]. Accordingly, EE has been used as a model to understand the brain-body connection and environmental stress inoculation which contributes to anti-obesity [1,2,11,13,14,16] and anti-cancer [2,9,11,45,46] phenotypes.

Primarily, our lab has applied EE to study brain-adipose interactions. We previously discovered that EE activates the HSA axis with hypothalamic BDNF as the key upstream brain mediator, leading to preferential sympathetic stimulation to WAT and subsequent adipose remodeling. This remodeling is characterized by leanness, lowered leptin levels, induction of beige cells in selective WAT depots, higher energy expenditure, and resistance to obesity [1,2]. In this study, we sought to elucidate and define additional downstream effectors of the HSA axis.

Our results show that EE-induced PTEN expression in WAT is associated with increased lipolysis, reduced fat mass, and reduced adipocyte area. PTEN upregulation in WAT as a consequence of the HSA axis is supported by several lines of evidence [1]: overexpressing BDNF in the hypothalamus upregulated adipose PTEN [2], BDNF heterozygous mice as well as TrkB.T1 inhibition of hypothalamic BDNF signaling downregulated adipose PTEN, and [3] β-blocker and 6OHDA-mediated denervation abolished EE-induced adipose PTEN upregulation—indicating the essential role of sympathetic innervation (Supplementary Fig. 3). Importantly, PTEN overexpression in WAT mimicked the shrink of adipose tissue seen in EE, whereas adipose PTEN knockdown blocked the EE-induced reduction in adipocyte size. Taken together, our data suggest PTEN may serve as one downstream mediator of the EE WAT phenotype, likely contributing to increased lipolysis and reduced adipocyte size.

In the 16-week EE experiment, WAT PTEN induction (Fig. 2E and F) was observed alongside decreased adiposity (Fig. 2C and D) and increased lean mass (Supplementary Fig. 1C). Overall, EE results in increased systemic glucose disposal (Fig. 2A and B). In contrast, no alterations in systemic glucose disposal were observed following PTEN overexpression (Fig. 4A) or PTEN knockdown in gWAT [25]. This implies local changes in WAT PTEN expression are insufficient to exert substantial influence on EE-mediated improvements in one marker of systemic metabolism, glucose disposal. These observations further implicate PTEN as a downstream effector of the HSA axis, enacting change at the local level as described above.

These data highlight the importance of the brain-body connection and the need for understanding of central control over peripheral processes. Previous data from our lab and others suggests that BDNF action within the arcuate (ARC), ventromedial (VMH), and dorsomedial (DMH) hypothalamus—whether through environmental or genetic means—leads to increased sympathetic outflow to adipose tissue, which yields increased levels of beta-adrenergic signaling and adipose browning in WAT [1,2,47,48]. Furthermore, recent work has described how BDNF action in the paraventricular nucleus (PVH) can alter leptin signaling and sympathetic architecture within peripheral adipose tissue, thus regulating energy homeostasis [49]. Further work will be necessary to elucidate the neural origin of anatomically discrete SNS efferent pathways and the environmental and genetic factors which lead to their activation.

Previous work by our lab has characterized downstream processes within the HSA axis, finding that EE-induced changes in downstream actors are not necessarily linked. For example, activation of the HSA axis both suppresses leptin expression—leading to anticancer effects [9]—and induces VEGF expression, resulting in beige cell induction in rWAT [15]. However, the leptin suppression and VEGF stimulation are dissociated, despite their occurrence downstream of adipocyte β-adrenergic signaling [1,2]. Future research will investigate additional functions of PTEN in responding to physiological cues provided by EE, and the crosstalk among adipose effectors downstream of the HSA axis. It will be important to delineate the local and systemic functions of these actors.

Few studies address the relationship between β-adrenergic signaling and PTEN in adipose tissue. Loss-of-function studies indicate that PTEN mediates adipocyte differentiation [21,22] and phosphorylation of HSL (S660)—the latter of which indicates PTEN is involved in lipolysis and thereby adipocyte size [25]. One study showed that β-adrenergic stimulation induced PTEN in T cells of adipose tissues, implicating a T-cell Stat6/PTEN in adipose function and maintenance [50].

The phosphoinositide 3-kinase (PI3K)/AKT pathway provides broader context for the connection between PTEN and lipolysis within WAT. PTEN participates in PI3K/AKT signaling pathway and negatively regulates PI3K activity and thus downstream AKT activation. AKT activation can suppress adipose lipolysis via phosphorylation and activation of various phosphodiesterase (PDE) isoforms, particularly PDE3B, which then degrades cyclic adenosine monophosphate (cAMP) and thereby inactivates protein kinase A (PKA). One downstream consequence is decreased phosphorylation of HSL and subsequent inhibition of lipolysis [51–54]. To this end, our previous [25] and current studies show that PTEN knockdown in WAT dramatically increased AKT phosphorylation, decreased downstream HSL phosphorylation, and increased adipocyte area.

PI3K p110α is the principal isoform that positively regulates insulin signaling. Araiz et al. reported that adipose-specific PI3K p110α inactivation potentiated β-adrenergic signaling, suggesting that PI3K inhibition within adipose tissue might improve the ability of β-adrenergic agonists to improve metabolic health [55]. Since PTEN acts to inhibit PI3K, it would follow that PTEN upregulation might potentiate the effect of β-adrenergic agonists. In fact, adipocyte overexpression of PTEN upregulated *Adrb3* expression (Fig. 4A). On the contrary, adipocyte knockdown of PTEN severely diminished *Adrb3* expression [25]. The link between PTEN and β-adrenergic signaling sensitivity warrants further investigation. With regard to EE, our lab has previously defined EE as a potent activator of β-adrenergic signaling via the HSA axis [1]. Interestingly, the sustained higher sympathetic tone in EE was associated with

a significant increase of *Adrb3* [1,2], a phenomenon not observed in chronic use of β3-agonist. The findings of this study intrigue us to ask whether EE activates β-adrenergic signaling on adipocytes via the HSA axis and thereby induces PTEN and subsequent suppression of PI3K, which in turn enhances β-adrenergic sensitivity. Future studies will investigate this hypothesized feed-forward cycle.

In addition, we observed that ERK phosphorylation was suppressed in WAT by EE and PTEN overexpression. *In vitro* experiments indicate that stimulation of β-adrenergic signaling activates ERK, thus promoting lipolysis [56,57], which contradict our *in vivo* findings. Differences in observations might be due to a temporal effect. EE housing occurs over weeks; in contrast, β-adrenergic stimulation in these cell culture studies was acute and transient. Previous work has shown that murine obesity models display increased ERK phosphorylation specifically in WAT. Additionally, sustained activation of the ERK pathway in adipocytes is associated with pathogenesis of type II diabetes [58,59]. Our previous studies have shown that EE is related with a reduced inflammatory response in adipose tissue [9,13]. Future investigation is required to assess the role of ERK pathway in EE-induced adipose remodeling including anti-inflammation.

Previous work using whole-body transgenic models of PTEN overexpression further support our findings. Two groups used a bacterial artificial chromosome transgenesis model to overexpress *Pten* approximately two-fold across many tissues [23,24]. Mild overexpression of *Pten* resulted in increased resistance to cancer, increased longevity, increased energy expenditure, and increased protection from insulin resistance and hepatosteatosis [23,24]. Unsurprisingly, systemic elevation of PTEN was also associated with inhibited PI3K/AKT signaling [23,24]. There are striking similarities between these germline global PTEN overexpression models and our physiological EE model. Our group and others have shown EE induce an anti-cancer and anti-obesity state across many murine disease models [1,2,9,11,45,46]. Our recent work suggests that implementing EE after middle age can increase healthspan [13,60]. We are excited to further investigate the adipose-specific contributions of PTEN toward local and systemic health.

In summary, here we show EE upregulates PTEN expression in WAT via the activation of the HSA axis. Adipocyte overexpression of PTEN suppresses AKT phosphorylation, enhances lipolysis, and reduces adipocyte size and adipose mass, recapitulating EE phenotypic changes. Knockdown of PTEN blocks the EE-induced reduction of adipocyte size. Together, our data highlight adipose PTEN as an important downstream mediator of a brain-adipose axis—the HSA axis—and further identify that PTEN contributes to the adipose remodeling process by responding to the social and physical stimuli provided by a complex environment.

## Author contributions

W.H. and N.J.Q. designed the studies, conducted experiments, interpreted the results, and wrote and revised the manuscript. T.B.M. designed the studies, conducted experiments, and interpreted the results. S.A. designed the adipocyte area algorithm and conducted experiments. R.K.W. and B.A. conducted experiments. L.C. conceived the concept, designed the studies, interpreted the results, and wrote and revised the manuscript.

## Declaration of Competing interest

L.C. and W.H. are inventors of a provisional patent application related to the liver-restricting AAV vector. All other authors declare no conflicts of interest.

## Acknowledgements

We would like to thank Run Xiao, Xianglan Liu, Jason J. Siu, Amber A. Boardman, and Brandon A. Sparks for technical assistance. This work was supported by NIH grants AG041250, CA166590, and CA163640 to L.C.

## Appendix A. Supplementary data

Supplementary data to this article can be found online at https://doi.org/10.1016/j.cpnec.2020.100013.

## References

[1] L. Cao, E.Y. Choi, X. Liu, A. Martin, C. Wang, X. Xu, M.J. During, White to brown fat phenotypic switch induced by genetic and environmental activation of a hypothalamic-adipocyte axis, Cell Metabol. 14 (2011) 324–338.
[2] L. Cao, X. Liu, E.J. Lin, C. Wang, E.Y. Choi, V. Riban, B. Lin, M.J. During, Environmental and genetic activation of a brain-adipocyte BDNF/leptin axis causes cancer remission and inhibition, Cell 142 (2010) 52–64.
[3] J. Nedergaard, B. Cannon, The browning of white adipose tissue: some burning issues, Cell Metabol. 20 (2014) 396–407.
[4] K.I. Stanford, R.J. Middelbeek, L.J. Goodyear, Exercise effects on white adipose tissue: beiging and metabolic adaptations, Diabetes 64 (2015) 2361–2368.
[5] J.B. Funcke, P.E. Scherer, Beyond adiponectin and leptin: adipose tissue-derived mediators of inter-organ communication, J. Lipid Res. 60 (2019) 1648–1684.
[6] A.M. Slater, L. Cao, A protocol for housing mice in an enriched environment, J Vis Exp (2015), e52874.
[7] L. Cao, M.J. During, What is the brain-cancer connection? Annu. Rev. Neurosci. 35 (2012) 331–345.
[8] J. Nithianantharajah, A.J. Hannan, Enriched environments, experience-dependent plasticity and disorders of the nervous system, Nat. Rev. Neurosci. 7 (2006) 697–709.
[9] G.D. Foglesong, N.J. Queen, W. Huang, K.J. Widstrom, L. Cao, Enriched environment inhibits breast cancer progression in obese models with intact leptin signaling, Endocr. Relat. Canc. 26 (5) (2019) 483–495.
[10] R. Xiao, S.M. Bergin, W. Huang, A.G. Mansour, X. Liu, R.T. Judd, K.J. Widstrom, N.J. Queen, R.K. Wilkins, J.J. Siu, S. Ali, M.A. Caligiuri, L. Cao, Enriched environment regulates thymocyte development and alleviates experimental autoimmune encephalomyelitis in mice, Brain Behav. Immun. 75 (2019) 137–148.
[11] R. Xiao, S.M. Bergin, W. Huang, A.M. Slater, X. Liu, R.T. Judd, E.D. Lin, K.J. Widstrom, S.D. Scoville, J. Yu, M.A. Caligiuri, L. Cao, Environmental and genetic activation of hypothalamic BDNF modulates T-cell immunity to exert an anticancer phenotype, Cancer Immunol Res 4 (2016) 488–497.
[12] S. Ali, X. Liu, N.J. Queen, R.S. Patel, R.K. Wilkins, X. Mo, L. Cao, Long-term environmental enrichment affects microglial morphology in middle age mice, Aging (N Y) 11 (2019) 2388–2402.
[13] T. McMurphy, W. Huang, X. Liu, J.J. Siu, N.J. Queen, R. Xiao, L. Cao, Implementation of environmental enrichment after middle age promotes healthy aging, Aging 10 (2018) 1698–1721.
[14] N.J. Queen, A.A. Boardman, R.S. Patel, J.J. Siu, X. Mo, L. Cao, Environmental enrichment improves metabolic and behavioral health in the BTBR mouse model of autism, Psychoneuroendocrinology 111 (2020), 104476.
[15] M.J. During, X. Liu, W. Huang, D. Magee, A. Slater, T. McMurphy, C. Wang, L. Cao, Adipose VEGF links the white-to-Brown fat switch with environmental, genetic, and pharmacological stimuli in male mice, Endocrinology 156 (2015) 2059–2073.
[16] X. Liu, T. McMurphy, R. Xiao, A. Slater, W. Huang, L. Cao, Hypothalamic gene transfer of BDNF inhibits breast cancer progression and metastasis in middle age obese mice, Mol. Ther. 22 (2014) 1275–1284.
[17] T. McMurphy, W. Huang, X. Liu, J.J. Siu, N.J. Queen, R. Xiao, L. Cao, Hypothalamic gene transfer of BDNF promotes healthy aging in mice, Aging Cell (2018), e12846.
[18] J. Li, C. Yen, D. Liaw, K. Podsypanina, S. Bose, S.I. Wang, J. Puc, C. Miliaresis, L. Rodgers, R. McCombie, S.H. Bigner, B.C. Giovanella, M. Ittmann, B. Tycko, H. Hibshoosh, M.H. Wigler, R. Parsons, PTEN, a putative protein tyrosine phosphatase gene mutated in human brain, breast, and prostate cancer, Science 275 (1997) 1943–1947.
[19] M.P. Myers, I. Pass, I.H. Batty, J. Van der Kaay, J.P. Stolarov, B.A. Hemmings, M.H. Wigler, C.P. Downes, N.K. Tonks, The lipid phosphatase activity of PTEN is critical for its tumor supressor function 95 (1998) 13513–13518.
[20] C. Kurlawalla-Martinez, B. Stiles, Y. Wang, S.U. Devaskar, B.B. Kahn, H. Wu, Insulin hypersensitivity and resistance to streptozotocin-induced diabetes in mice lacking PTEN in adipose tissue, Mol. Cell Biol. 25 (2005) 2498–2510.
[21] T.S. Morley, J.Y. Xia, P.E. Scherer, Selective enhancement of insulin sensitivity in the mature adipocyte is sufficient for systemic metabolic improvements, Nat. Commun. 6 (2015) 7906.
[22] J. Sanchez-Gurmaches, C.M. Hung, C.A. Sparks, Y. Tang, H. Li, D.A. Guertin, PTEN loss in the Myf5 lineage redistributes body fat and reveals subsets of white adipocytes that arise from Myf5 precursors, Cell Metabol. 16 (2012) 348–362.
[23] A. Ortega-Molina, A. Efeyan, E. Lopez-Guadamillas, M. Munoz-Martin, G. Gomez-Lopez, M. Canamero, F. Mulero, J. Pastor, S. Martinez, E. Romanos, M. Mar Gonzalez-Barroso, E. Rial, A.M. Valverde, J.R. Bischoff, M. Serrano, Pten positively regulates brown adipose function, energy expenditure, and longevity, Cell Metabol. 15 (2012) 382–394.
[24] I. Garcia-Cao, M.S. Song, R.M. Hobbs, G. Laurent, C. Giorgi, V.C. de Boer, D. Anastasiou, K. Ito, A.T. Sasaki, L. Rameh, A. Carracedo, M.G. Vander Heiden, L.C. Cantley, P. Pinton, M.C. Haigis, P.P. Pandolfi, Systemic elevation of PTEN induces a tumor-suppressive metabolic state, Cell 149 (2012) 49–62.
[25] W. Huang, N.J. Queen, T.B. McMurphy, S. Ali, L. Cao, Adipose PTEN regulates adult adipose tissue homeostasis and redistribution via a PTEN-leptin-sympathetic loop, Mol Metab 30 (2019) 48–60.

[26] M. Katic, A.R. Kennedy, I. Leykin, A. Norris, A. McGettrick, S. Gesta, S.J. Russell, M. Bluher, E. Maratos-Flier, C.R. Kahn, Mitochondrial gene expression and increased oxidative metabolism: role in increased lifespan of fat-specific insulin receptor knock-out mice, Aging Cell 6 (2007) 827–839.
[27] M. Bluher, M.D. Michael, O.D. Peroni, K. Ueki, N. Carter, B.B. Kahn, C.R. Kahn, Adipose tissue selective insulin receptor knockout protects against obesity and obesity-related glucose intolerance, Dev. Cell 3 (2002) 25–38.
[28] M. Bluher, B.B. Kahn, C.R. Kahn, Extended longevity in mice lacking the insulin receptor in adipose tissue, Science 299 (2003) 572–574.
[29] X. Liu, D. Magee, C. Wang, T. McMurphy, A. Slater, M. During, L. Cao, Adipose tissue insulin receptor knockdown via a new primate-derived hybrid recombinant AAV serotype, Molecular Therapy - Methods & Clinical Development 1 (2014) 8.
[30] W. Huang, X. Liu, N.J. Queen, L. Cao, Targeting visceral fat by intraperitoneal delivery of novel AAV serotype vector restricting off-target transduction in liver, Mol Ther Methods Clin Dev 6 (2017) 68–78.
[31] Y. Zhu, Y. Gao, C. Tao, M. Shao, S. Zhao, W. Huang, T. Yao, J.A. Johnson, T. Liu, A.M. Cypess, O. Gupta, W.L. Holland, R.K. Gupta, D.C. Spray, H.B. Tanowitz, L. Cao, M.D. Lynes, Y.H. Tseng, J.K. Elmquist, K.W. Williams, H.V. Lin, P.E. Scherer, Connexin 43 mediates white adipose tissue beiging by facilitating the propagation of sympathetic neuronal signals, Cell Metabol. 24 (2016) 420–433.
[32] R. Ng, N.A. Hussain, Q. Zhang, C. Chang, H. Li, Y. Fu, L. Cao, W. Han, W. Stunkel, F. Xu, miRNA-32 drives Brown fat thermogenesis and trans-activates subcutaneous white fat browning in mice, Cell Rep. 19 (2017) 1229–1246.
[33] Y. Zhang, L. Xie, S.K. Gunasekar, D. Tong, A. Mishra, W.J. Gibson, C. Wang, T. Fidler, B. Marthaler, A. Klingelhutz, E.D. Abel, I. Samuel, J.K. Smith, L. Cao, R. Sah, SWELL1 is a regulator of adipocyte size, insulin signalling and glucose homeostasis, Nat. Cell Biol. 19 (2017) 504–517.
[34] R. Xiao, A.G. Mansour, W. Huang, L.A. Chrislip, R.K. Wilkins, N.J. Queen, Y. Youssef, H.C. Mao, M.A. Caligiuri, L. Cao, Adipocytes: a novel target for IL-15/IL-15Ralpha cancer gene therapy, Mol. Ther. 27 (2019) 922–932.
[35] L. Cao, X. Jiao, D.S. Zuzga, Y. Liu, D.M. Fong, D. Young, M.J. During, VEGF links hippocampal activity with neurogenesis, learning and memory, Nat. Genet. 36 (2004) 827–835.
[36] P. Charbel Issa, S.R. De Silva, D.M. Lipinski, M.S. Singh, A. Mouravlev, Q. You, A.R. Barnard, M.W. Hankins, M.J. During, R.E. Maclaren, Assessment of tropism and effectiveness of new primate-derived hybrid recombinant AAV serotypes in the mouse and primate retina, PloS One 8 (2013), e60361.
[37] W. Huang, N.J. Queen, L. Cao, rAAV-mediated gene delivery to adipose tissue, Methods Mol. Biol. (2019) 389–405.
[38] W.E. Lyons, L.A. Mamounas, G.A. Ricaurte, V. Coppola, S.W. Reid, S.H. Bora, C. Wihler, V.E. Koliatsos, L. Tessarollo, Brain-derived neurotrophic factor-deficient mice develop aggressiveness and hyperphagia in conjunction with brain serotonergic abnormalities, Proc. Natl. Acad. Sci. U.S.A. 96 (1999) 15239–15244.
[39] A. Konkle, A.C. Kentner, S.L. Baker, A. Stewart, C. Bielajew, Environmental-enrichment–related variations in behavioral, biochemical, and physiologic responses of Sprague–Dawley and Long Evans rats, JAALAS 49 (2010) 427–436.
[40] I.A.S. Olsson, K. Dahlborn, Improving housing conditions for laboratory mice: a review of environmental enrichment 36, Laboratory animals, 2002, pp. 243–270.
[41] F. Larsson, B. Winblad, A.H. Mohammed, Psychological stress and environmental adaptation in enriched vs. impoverished housed rats, Pharmacol. Biochem. Behav. 73 (2002) 193–207.
[42] N. Benaroya-Milshtein, N. Hollander, A. Apter, T. Kukulansky, N. Raz, A. Wilf, I. Yaniv, C.G. Pick, Environmental enrichment in mice decreases anxiety, attenuates stress responses and enhances natural killer cell activity, Eur. J. Neurosci. 20 (2004) 1341–1347.
[43] C. Fox, Z. Merali, C. Harrison, Therapeutic and protective effect of environmental enrichment against psychogenic and neurogenic stress, Behav. Brain Res. 175 (2006) 1–8.
[44] J.E. Sparling, S.L. Baker, C. Bielajew, Effects of combined pre-and post-natal enrichment on anxiety-like, social, and cognitive behaviours in juvenile and adult rat offspring, Behav. Brain Res. 353 (2018) 40–50.
[45] G. Li, Y. Gan, Y. Fan, Y. Wu, H. Lin, Y. Song, X. Cai, X. Yu, W. Pan, M. Yao, J. Gu, H. Tu, Enriched environment inhibits mouse pancreatic cancer growth and down-regulates the expression of mitochondria-related genes in cancer cells, Sci. Rep. 5 (2015) 7856.
[46] B.D. Bice, M.R. Stephens, S.J. Georges, A.R. Venancio, P.C. Bermant, A.V. Warncke, K.E. Affolter, J.R. Hidalgo, M.L. Angus-Hill, Environmental enrichment induces pericyte and IgA-dependent wound repair and lifespan extension in a colon tumor model, Cell Rep. 19 (2017) 760–773.
[47] T.J. Unger, G.A. Calderon, L.C. Bradley, M. Sena-Esteves, M. Rios, Selective deletion of Bdnf in the ventromedial and dorsomedial hypothalamus of adult mice results in hyperphagic behavior and obesity, J. Neurosci. 27 (2007) 14265–14274.
[48] C. Wang, E. Bomberg, C.J. Billington, A.S. Levine, C.M. Kotz, Brain-derived neurotrophic factor (BDNF) in the hypothalamic ventromedial nucleus increases energy expenditure, Brain Res. 1336 (2010) 66–77.
[49] P. Wang, K.H. Loh, M. Wu, D.A. Morgan, M. Schneeberger, X. Yu, J. Chi, C. Kosse, D. Kim, K. Rahmouni, P. Cohen, J. Friedman, A leptin–BDNF pathway regulating sympathetic innervation of adipose tissue, Nature 583 (2020) 839–844.
[50] S. Kalin, M. Becker, V.B. Ott, I. Serr, F. Hosp, M.M.H. Mollah, S. Keipert, D. Lamp, F. Rohner-Jeanrenaud, V.K. Flynn, M.G. Scherm, L.F.R. Nascimento, K. Gerlach, V. Popp, S. Dietzen, T. Bopp, P. Krishnamurthy, M.H. Kaplan, M. Serrano, S.C. Woods, P. Tripal, R. Palmisano, M. Jastroch, M. Bluher, C. Wolfrum, B. Weigmann, A.G. Ziegler, M. Mann, M.H. Tschop, C. Daniel, A stat6/pten Axis links regulatory T cells with adipose tissue function, Cell Metabol. 26 (2017) 475–492.e7.
[51] C. Berggreen, A. Gormand, B. Omar, E. Degerman, O. Goransson, Protein kinase B activity is required for the effects of insulin on lipid metabolism in adipocytes, Am. J. Physiol. Endocrinol. Metab. 296 (2009) E635–E646.
[52] T. Kitamura, Y. Kitamura, S. Kuroda, Y. Hino, M. Ando, K. Kotani, H. Konishi, H. Matsuzaki, U. Kikkawa, W. Ogawa, M. Kasuga, Insulin-induced phosphorylation and activation of cyclic nucleotide phosphodiesterase 3B by the serine-threonine kinase Akt, Mol. Cell Biol. 19 (1999) 6286–6296.
[53] P.B. Snyder, J.M. Esselstyn, K. Loughney, S.L. Wolda, V.A. Florio, The role of cyclic nucleotide phosphodiesterases in the regulation of adipocyte lipolysis, J. Lipid Res. 46 (2005) 494–503.
[54] Y.H. Choi, S. Park, S. Hockman, E. Zmuda-Trzebiatowska, F. Svennelid, M. Haluzik, O. Gavrilova, F. Ahmad, L. Pepin, M. Napolitano, M. Taira, F. Sundler, L. Stenson Holst, E. Degerman, V.C. Manganiello, Alterations in regulation of energy homeostasis in cyclic nucleotide phosphodiesterase 3B-null mice, J. Clin. Invest. 116 (2006) 3240–3251.
[55] C. Araiz, A. Yan, L. Bettedi, I. Samuelson, S. Virtue, A.K. McGavigan, C. Dani, A. Vidal-Puig, L.C. Foukas, Enhanced β-adrenergic signalling underlies an age-dependent beneficial metabolic effect of PI3K p110α inactivation in adipose tissue, Nat. Commun. 10 (2019) 1546.
[56] A.S. Greenberg, W.J. Shen, K. Muliro, S. Patel, S.C. Souza, R.A. Roth, F.B. Kraemer, Stimulation of lipolysis and hormone-sensitive lipase via the extracellular signal-regulated kinase pathway, J. Biol. Chem. 276 (2001) 45456–45461.
[57] S. Collins, Beta-adrenoceptor signaling networks in adipocytes for recruiting stored fat and energy expenditure, Front. Endocrinol. 2 (2011) 102.
[58] S. Hong, W. Song, P.H. Zushin, B. Liu, M.P. Jedrychowski, A.I. Mina, Z. Deng, D. Cabarkapa, J.A. Hall, C.J. Palmer, H. Aliakbarian, J. Szpyt, S.P. Gygi, A. Tavakkoli, L. Lynch, N. Perrimon, A.S. Banks, Phosphorylation of Beta-3 adrenergic receptor at serine 247 by ERK MAP kinase drives lipolysis in obese adipocytes, Mol Metab 12 (2018) 25–38.
[59] K.I. Ozaki, M. Awazu, M. Tamiya, Y. Iwasaki, A. Harada, S. Kugisaki, S. Tanimura, M. Kohno, Targeting the ERK signaling pathway as a potential treatment for insulin resistance and type 2 diabetes, Am. J. Physiol. Endocrinol. Metab. 310 (2016) E643–E651.
[60] N.J. Queen, Q.N. Hassan, L. Cao, Improvements to healthspan through environmental enrichment and lifestyle interventions: where are we now? Front. Neurosci. 14 (2020) 605.